

Article

A Metamaterial Solution for Soundproofing on Board Ship

Giada Kyaw Oo D'Amore ^{1,*} , Stefano Caverni ^{2,3}, Marco Biot ¹, Giovanni Rognoni ¹ and Luca D'Alessandro ²

¹ Engineering and Architecture Department, University of Trieste, 34127 Trieste, Italy; biot@units.it (M.B.); giovanni.rognoni@phd.units.it (G.R.)

² Phononic Vibes Srl, 20158 Milano, Italy; stefano.caverni@phononicvibes.com (S.C.); luca.dalessandro@phononicvibes.com (L.D.)

³ Civil and Environmental Engineering, Politecnico di Milano, 20133 Milano, Italy

* Correspondence: giada.kyawood'amore@phd.units.it

Featured Application: In this work a new metamaterial solution is proven to be a valid substitute for the traditional solutions adopted on board for soundproofing.

Abstract: The design of innovative metamaterials with robust and reliable performances is attracting increasing interest in shipbuilding, due to the potential and versatility of these materials. In particular, soundproofing is becoming an even more important characteristic, to ensure the comfort levels required by the standards on board ships. Thus, shipyards are constantly looking for innovative solutions to improve the insulation between environments, while respecting the safety regulations with which the materials on board must comply. In this study, an innovative solution called the Metasolution is designed and characterized, considering both the transmission loss (TL) and the fire resistance. The Metasolution is proven to be a valid substitute for the traditional honeycomb panels used on board for soundproofing. The TL of the innovative solution is increased, and the thickness is decreased, while maintaining the cost and the weight in line with the traditional solution. Moreover, the regulations regarding fire safety on board are satisfied.

Keywords: metamaterials; sound transmission loss; fire resistance; shipbuilding



Citation: Kyaw Oo D'Amore, G.; Caverni, S.; Biot, M.; Rognoni, G.; D'Alessandro, L. A Metamaterial Solution for Soundproofing on Board Ship. *Appl. Sci.* **2022**, *12*, 6372. <https://doi.org/10.3390/app12136372>

Academic Editor: Qingbo He

Received: 18 May 2022

Accepted: 21 June 2022

Published: 23 June 2022

Publisher's Note: MDPI stays neutral with regard to jurisdictional claims in published maps and institutional affiliations.



Copyright: © 2022 by the authors. Licensee MDPI, Basel, Switzerland. This article is an open access article distributed under the terms and conditions of the Creative Commons Attribution (CC BY) license (<https://creativecommons.org/licenses/by/4.0/>).

1. Introduction

Traditional noise reduction partitions can rely on the mass law principle (soundproofing is achieved by using dense material or by increasing thickness) showing a 6 dB per octave band increase in the sound transmission loss (STL) [1,2].

Alternatively, mass–spring–mass (MSM) or mass–air–mass (MAM) solutions are usually more effective, with higher insulation performances and mass savings [3,4]. The transmission loss curve of such multi-layered systems shows a higher slope (from 16 to 18 dB per octave band) over a wide frequency range, but presents a performance drop in the low-frequency range due to the system resonance [5–7].

In this framework, further sound insulation performance improvement can be achieved by adopting innovative solutions based on metamaterial physics.

Acoustic metamaterials are materials engineered to control, direct, and manipulate sound waves, by transmitting, trapping, and amplifying the sound waves at certain frequencies [8–14]. This outcome is usually achieved by the periodic repetition in space of an elementary primitive cell, carefully optimized in its topology and geometry [4,8,13–15]. The repetition in geometry can be achieved by adding masses connected with a suitably chosen stiffness [16,17], through notches on the surface of the plate [7,12] or with an open aperture on a hollow cavity [18] or labyrinthine path [19].

In a certain frequency range, acoustic metamaterials can significantly reduce the transmission of sound waves through their structure. To extend this improvement range,

metamaterials with different characteristic can be layered. These properties make acoustic metamaterials an effective and lightweight solution for noise and vibration proofing [3,9].

In the aeronautical field, the effect of different metamaterial solutions (i.e., structures composed of primitive cells repeated in space) for the core of sandwich panels has been numerically and theoretically studied [19–21], as an improvement to the traditional honeycomb core solution from a structural, weight, and STL performance point of view. This involves the repetition in space of different morphologies of lattice structures: pyramidal truss cores [19,20], two-layered pyramidal truss cores [21], tetrahedral cores [19], and 3D Kagome cores [20]. These types of solutions can be redirected to the MAM and MSM typologies of metamaterials, thus presenting a new solution.

This work aims to introduce a novel metamaterial solution (the Metasolution in the following) and a related design approach for noise reduction applications, proposing a new lattice structure for sandwich panels, focusing on the on-board-ship environment with all its regulations and constraints.

The target acoustic performance, weight and thickness are set by the traditional solution usually adopted in this sector, composed of two honeycomb aluminum panels and a mineral wool layer. Its STL is determined from the experimental point of view in coupled chambers in the laboratory, using a sound intensity measurement technique.

The innovative metamaterial solution is then optimized to exceed the sound insulation performances offered by traditional solutions, reducing the panel thickness while keeping weight and costs constant.

The Metasolution is designed using an FEM acoustic–structural numerical model, and the model is validated by comparing the numerically predicted acoustic performances with the performed experimental test. To ensure that the Metasolution is compliant with the safety regulations imposed for materials on board [22], the surface flammability and the spread of flame are also evaluated.

In the following sections:

1. The traditional honeycomb panel solution is presented and characterized experimentally to determine its STL.
2. The description of materials and geometries and the numerical method adopted for the design of the metamaterial solution are shown, together with its predicted performances.
3. The STL of the optimized Metasolution is also measured experimentally, and a comparison with the benchmark standard partition is made.
4. Finally, the surface flammability and the spread of flame of the prototype are evaluated.

2. Benchmark Solution for Sound Insulation on Board

A standard solution for noise insulation on board ship is considered to set a benchmark in terms of acoustic performance, weight, and thickness. The panel is composed of a couple of aluminum honeycomb panels and a mineral wool layer (Figure 1).



Figure 1. Traditional solution components: (a) honeycomb aluminum panels; (b) mineral wool layer.

Figure 2 shows the prototype mounted in the acoustically coupled chambers to measure its STL according to ISO 15186 1–2 [23,24]. The panel, with dimensions of 800×800 mm, was installed on the test window between the reverberant and the hemi-anechoic chamber, with mastic used for sealing. The reverberant room had a volume of 252 m^3 and was equipped with a tetrahedral source of the Genelec 8351A type and six B&K 1/4" type 4135 microphones. The sound power in the receiving room (hemi-anechoic chamber) was measured using a B&K sound intensity PP type 2681 probe. The weighted sound reduction index (R_w) was evaluated according to ISO 717-1 [25], leading to the value of R_w (Figure 3) used as a benchmark. Since the results cannot be explicitly reported for confidentiality reasons, only the 10 dB increase is reported on the ordinate axis.

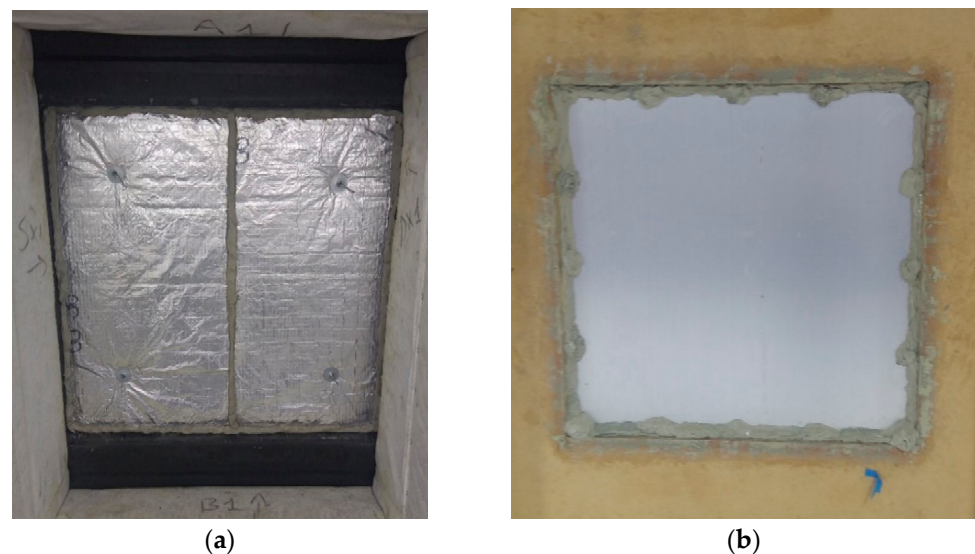


Figure 2. Experimental setup for STL measurement for benchmark solution: (a) hemi-anechoic chamber side view (mineral wool side); (b) reverberant room side view (honeycomb aluminum panel side).

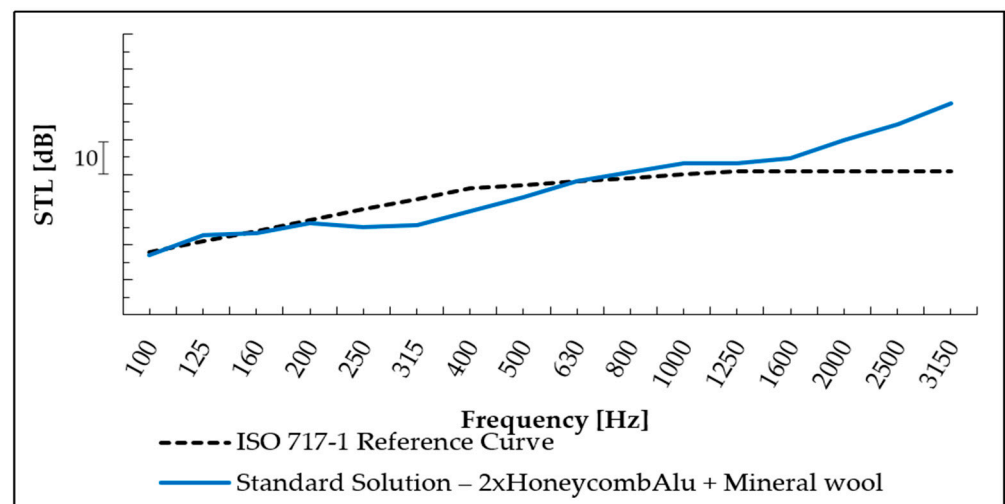


Figure 3. Benchmark solution experimental STL and ISO 717-1 reference curve for R_w calculation.

3. Metamaterial Solution: Materials, Methods, and Design

In the following sections, the metamaterial panel developed in this study is presented. Its acoustic performances are evaluated and optimized via FEM analysis, and both the numerical methodology and the results are addressed.

3.1. Metasolution Geometry

The Metasolution is composed of a periodic structure with an in-plane repetition of a primitive cell (Figure 4). The unit cell consists of two mass elements and a series of internal beam connections. The geometry of the primitive cell is composed of three main elements: two panels (mass elements) and a system of beams connecting the two panels (spring equivalent element). The system is composed of 4 S-shaped beams which connect the external part of the first panel to the inner area of the second panel.

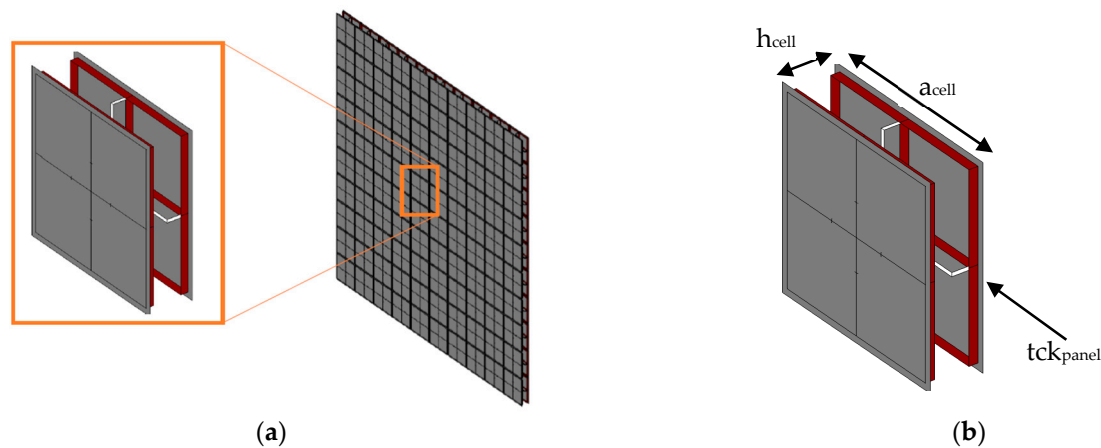


Figure 4. (a) Elementary cell detail extracted from periodic Metasolution and (b) characteristic dimensions.

From the dynamic point of view, the mass elements work with a rigid body motion, and the beam-like connections deform in bending, giving an MSM type of behavior to the solution that leads to optimal sound insulation performance over a wide frequency range.

In the design process, particular attention was paid to the resonance-dominated region of the STL and to the interaction between the mechanical and air stiffness inside the panel (MAM behavior). The internal beams are dimensioned to give the solution a self-standing capacity, at the same time avoiding excessive stiffening of the structure, and therefore not affecting the acoustic performance in the medium–low frequency range.

The unit cell is made of steel, with properties as listed in Table 1.

Table 1. Steel physical properties.

E [GPa]	ν [-]	ρ [kg/m ³]	η [-]
210	0.3	7850	0.05

E: Young's modulus; ν : Poisson coefficient; ρ : density; η : loss factor.

3.2. Numerical Method

The STL performances of the Metasolution were numerically evaluated and optimized by means of a plane-wave tube model. The model was implemented by adopting the Acoustics Pressure Module coupled with the Solid Mechanics Module of COMSOL Multiphysics v5.6.

With this numerical approach, a single unit cell is modeled, saving a significant amount of computational effort. The performances of a complete periodic panel of size 800 × 800 mm were derived by applying the Bloch–Floquet boundary conditions [26].

The Bloch–Floquet wave vector corresponds to the wave vector of the incident wave

$$k_{in} = [k_{x,in}, k_{y,in}, k_{z,in}] = [k_0 \sin \theta \cos \Phi, k_0 \sin \theta \cos \Phi, k_0 \cos \Phi] \quad (1)$$

where k_0 is the wave number of the fluid, θ is the incidence angle, and Φ is the azimuth angle of the applied incident wave.

According to [6], the diffuse field transmission coefficient for a finite-dimensions panel is:

$$\tau_{diff,fin} = \left(\frac{\int_0^{\theta_{lim}} \tau_{fin}(\theta) \cos \theta \sin \theta d\theta}{\int_0^{\theta_{lim}} \cos \theta \sin \theta d\theta} \right) \quad (2)$$

The τ_{fin} term is the transmission coefficient calculated as:

$$\tau_{fin}(\theta) = \tau_{inf}(\theta) \sigma_{R,avg} \cos \theta \quad (3)$$

where τ_{inf} is the transmission coefficient for a panel with infinite dimensions, which can be easily determined from the numerical model with imposed periodic boundary conditions on the unit cell. Considering the relation between the STL for an infinite panel in a diffuse sound field and the transmission coefficient:

$$STL_{inf}(\theta) = 10 \log_{10} \left(\frac{1}{\tau_{inf}(\theta)} \right) \quad (4)$$

and combining Equations (2)–(4), the STL for a finite panel in a diffuse sound field can be derived:

$$STL_{diff,fin} = -10 \log_{10}(\tau_{diff,fin}) = -10 \log_{10} \left(\frac{\int_0^{\theta_{lim}} \tau_{inf}(\theta) \sigma_{R,avg} \cos^2 \theta \sin \theta d\theta}{\int_0^{\theta_{lim}} \cos \theta \sin \theta d\theta} \right) \quad (5)$$

where $\sigma_{R,avg}$ is the averaged geometrical efficiency, calculated as a function of the incidence angle for the different frequencies as:

$$\sigma_{R,avg} = \left(\frac{Re\{Z_r\}}{Z_0} \right) \quad (6)$$

and Z_0 is the characteristic impedance of air. Z_r is the radiation impedance of the acoustic panel, which is evaluated according to the methodology proposed in [27].

3.3. FEM-Simulated STL of Metasolution

The numerical tool described in the previous section was used to perform an extensive numerical analysis of the Metasolution, in order to efficiently design the geometry before prototyping.

A series of simulations was carried out by varying the characteristic dimensions of the unit cell alternately, while keeping the others constant. The dimensions chosen for the optimization are reported in Table 2.

Table 2. Values chosen for primitive unit cell characteristic dimensions (with reference to Figure 4b) used for the optimization process, with corresponding Rw.

Variable	a_{cell} [mm]	tck_{panel} [mm]	h_{cell} [mm]	Rw [dB]
h_{cell}	150	1.0	35	+4
			40	+6
			45	+5
			50	+5
a_{cell}	100	1.0	40	+5
	120			+5
	150			+6
tck_{panel}	150	0.7	40	−1
		0.8		+3
		1.0		+6
		1.2		+7

a_{cell} : cell width; tck_{panel} : panel thickness; h_{cell} : cell height.

The results in terms of STL for each of the three groups of simulations are represented in Figures 5–7, and the ΔR_w values calculated with respect to the benchmark solution value for each configuration are reported in Table 2. Since the results cannot be explicitly reported for confidentiality reasons, only the 10 dB increase is reported on the ordinate axis, so that a comparison between the curves is still possible.

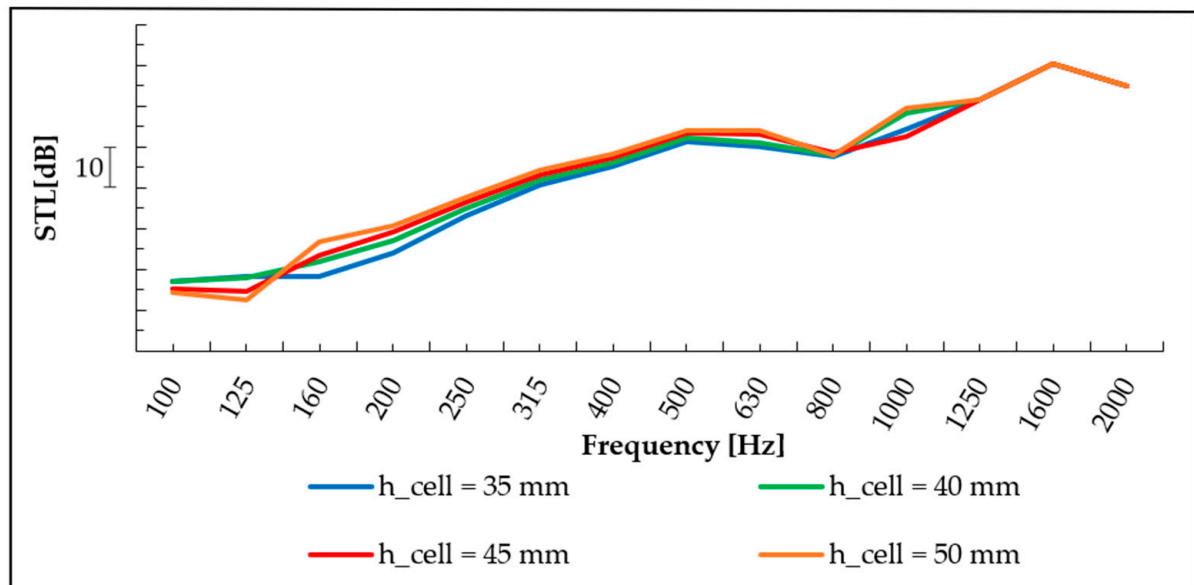


Figure 5. STL numerical results keeping the nominal dimensions for a_{cell} and $t_{\text{ck}_{\text{panel}}}$ and varying h_{cell} .

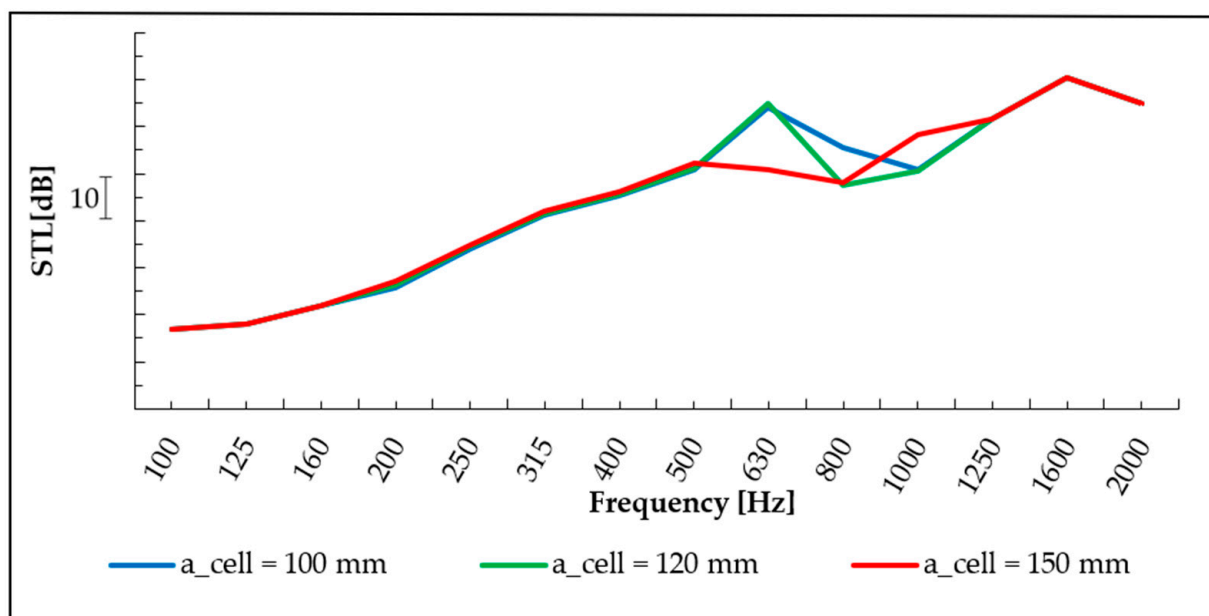


Figure 6. STL numerical results keeping the nominal dimensions for $t_{\text{ck}_{\text{panel}}}$ and h_{cell} and varying a_{cell} .

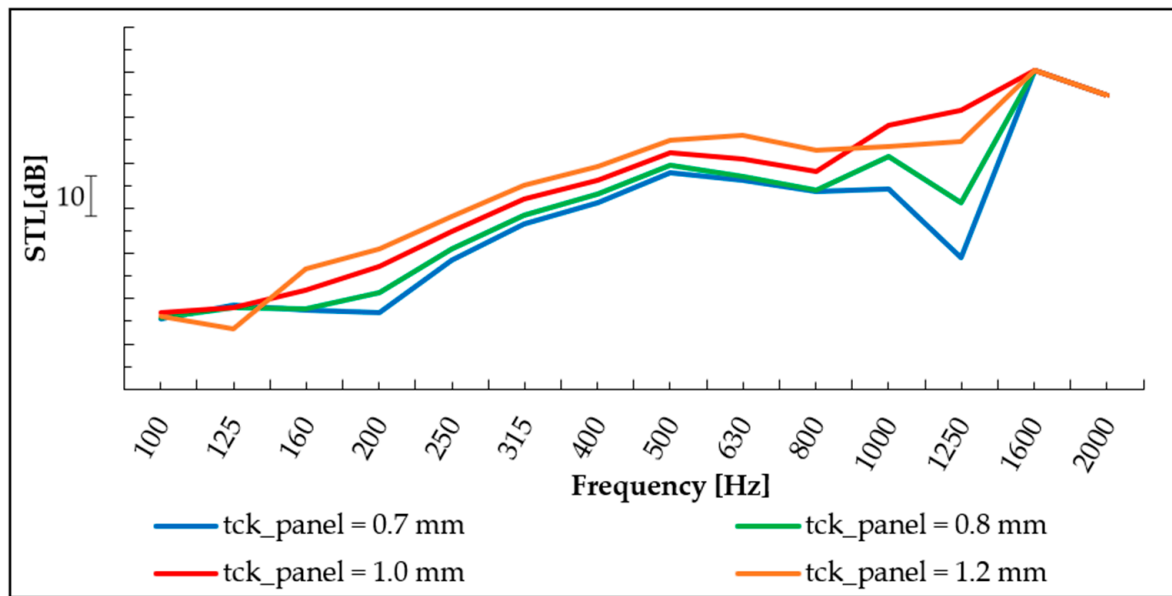


Figure 7. STL numerical results keeping the nominal dimensions for a_{cell} and h_{cell} and varying $t_{\text{ck_panel}}$.

The configuration reported in Table 3 was chosen as the best one in terms of both STL and ΔR_w .

Table 3. Unit cell geometrical dimensions.

$t_{\text{ck_panel}}$ [mm]	a_{cell} [mm]	h_{cell} [mm]	A_w [kg/m ²]	R_w [dB]
1	150	40	18.5	43

4. Experimental Sound Transmission Loss Results

In the following sections, the prototyping of the optimized Metasolution is shown, the STL measured in a double chamber test is addressed, and a practical application of the Metasolution as a ceiling covering on board ship is analyzed.

4.1. Prototyping and Double Chamber Experimental Test

The unit cells with dimensions reported in Table 3 were manufactured and arranged to create the periodic structure. The Metasolution was finished by fixing two steel plates outside the elastic structure, as shown in Figure 8.



Figure 8. Tested Metasolution sample consisting of the combination of elastic structure and external steel panels.

The prototype was tested in a double chamber, using the same setup used for the benchmark solution (Section 2). The measured STL is reported in Figure 9 and compared with the numerical STL. The experimental results match the overall trend of the numerical curve, ensuring the accuracy of the FEM model used for the optimization.

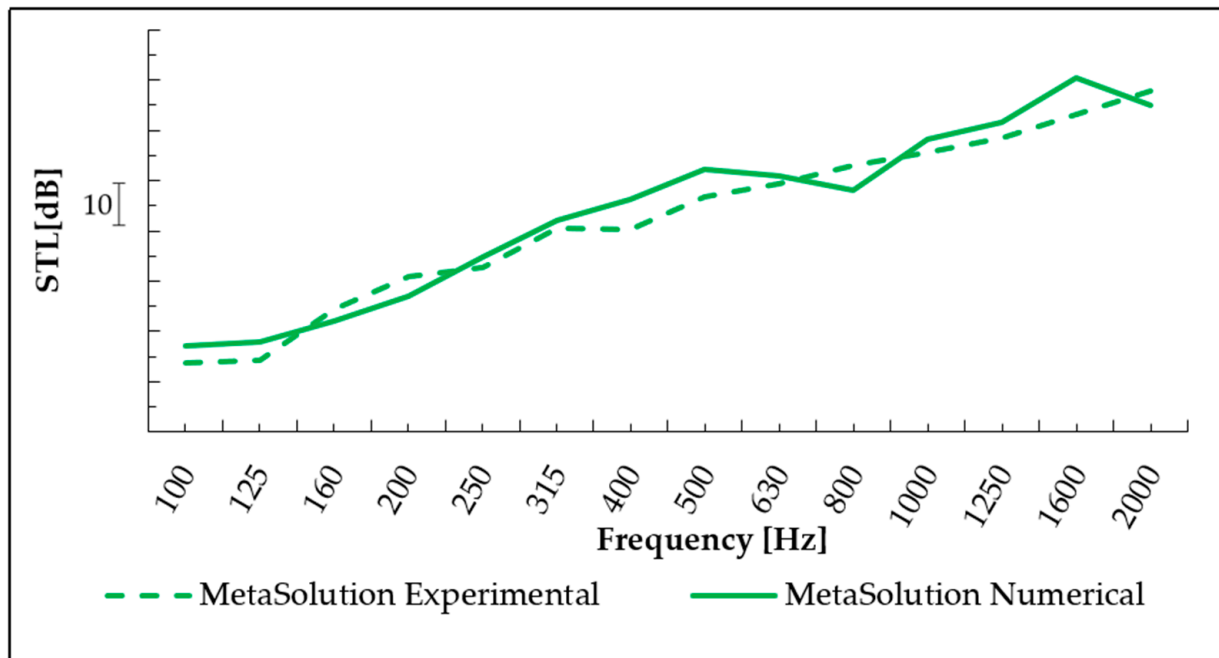


Figure 9. Numerical vs. experimental STL for Metasolution.

Figure 10 shows the comparison between the benchmark solution and the Metasolution experimental STLs. The Metasolution has a higher STL than the benchmark solution, except in the frequency range of 100–160 Hz. Moreover, the Metasolution achieves an ΔR_w higher than 6 dB with respect to the benchmark solution.

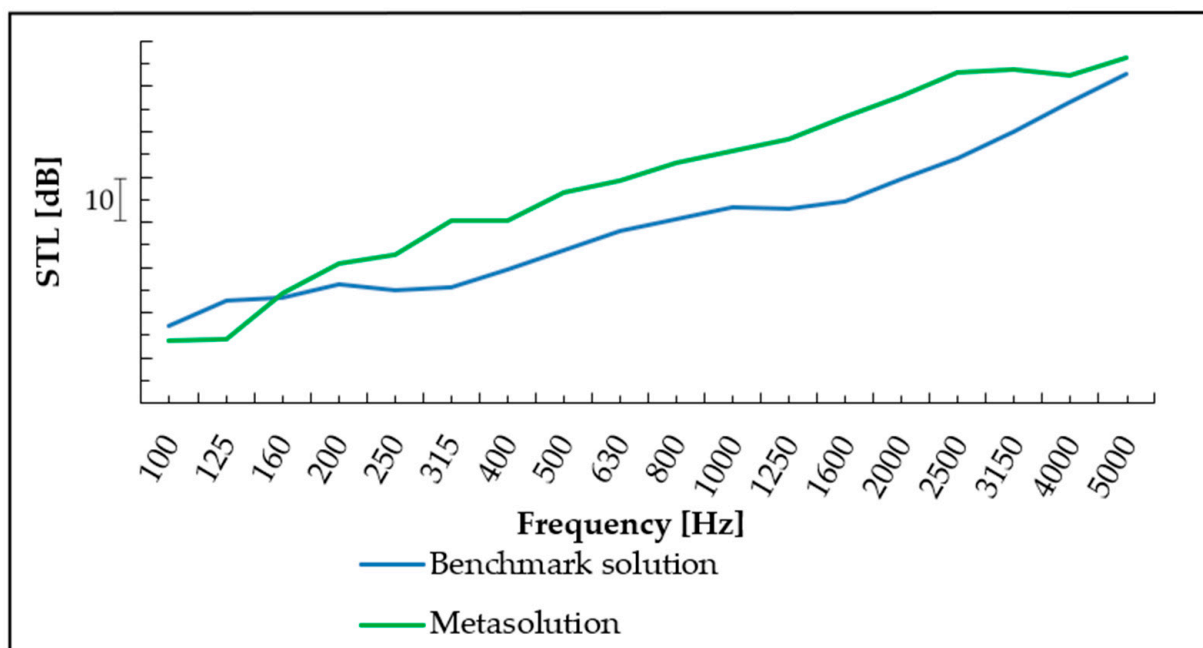


Figure 10. Metasolution vs. benchmark solution experimental STLs.

4.2. Real-Case Scenario on Board: Ceiling Covering

The optimized Metasolution was mounted and tested in a real-case scenario representative of applications on board ship, as a ceiling covering for acoustic insulation between decks. Two different configurations were chosen for testing, varying the distance of the sound insulation panel from the ceiling. The first configuration had an air gap between the panel and the ceiling, and the second one had no air gap (Figure 11).

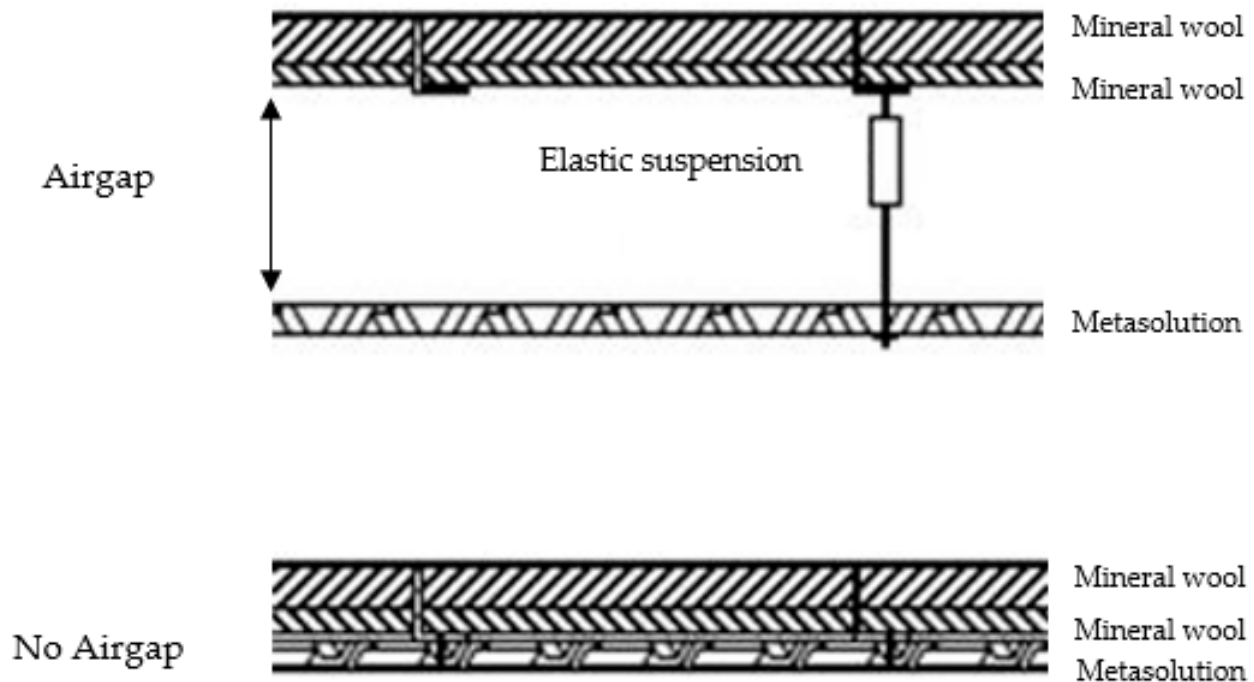


Figure 11. Scheme of the deck covering assembly in the two configurations (image adapted from technical report).

The solution was fixed to the ceiling (covered with two layers of mineral wool of different heights) with elastic suspensions (Figures 11 and 12).



Figure 12. Deck covering mock-up with the 450 mm air-gap configuration.

In these configurations, the R_w was evaluated by performing sound transmission loss measurements, with the sound source placed in the room under the ceiling and the receiving microphones located in the room above the deck.

The R_w of the Metasolution in the first configuration was higher by 6 dB with respect to the R_w in the second configuration (Figure 13). These values broadly satisfy the limit reported in the Code On Noise Levels On Board Ships [22] in cabins.

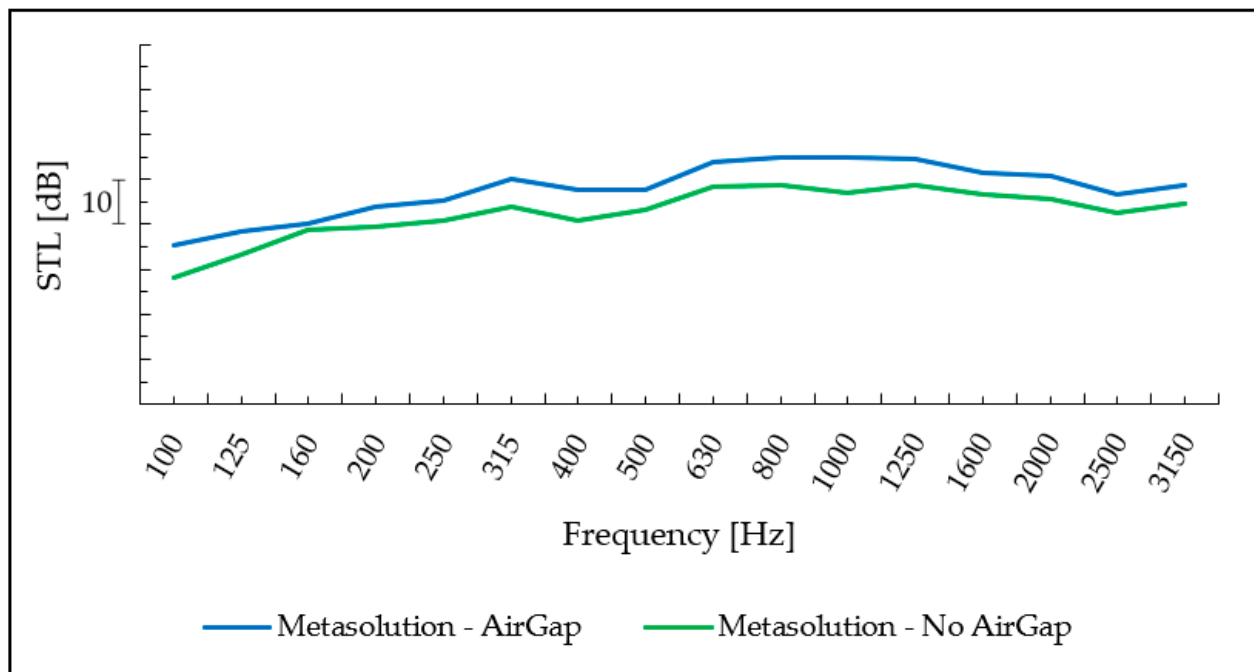


Figure 13. Experimental results for the Metasolution tested with different air gaps.

5. Surface Flammability and Spread of Flame

In this section, the test carried out to ensure the compliance of the Metasolution with safety regulations [22] is presented. For the test, the inner core of the Metasolution was prototyped in recycled plastic material and carefully dimensioned to maintain the same acoustic performances as the original steel solution, to analyze an alternative version of the solution representing the worst-case scenario for fire resistance (Figure 14).

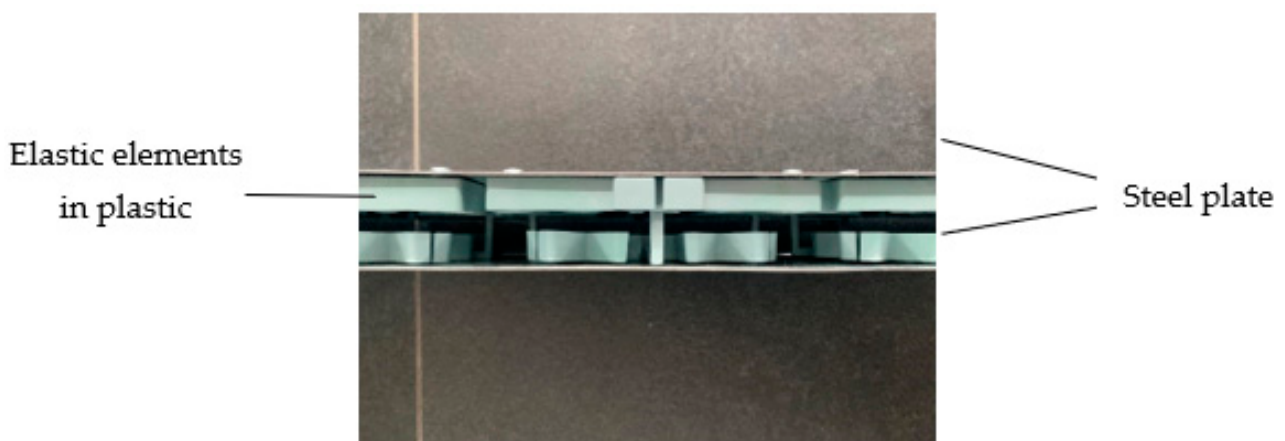


Figure 14. Metasolution with elastic elements in recycled plastic.

Two samples were tested, and the tests were performed in accordance with the guidelines reported in the FTP Code [28–30]. The test method consists of exposing the specimen to a well-defined radiated heat flux generated by a gas-fired panel. A pilot flame is sited close to the hotter end of the specimen to ignite the volatile gases issuing from the surface (Figure 15).

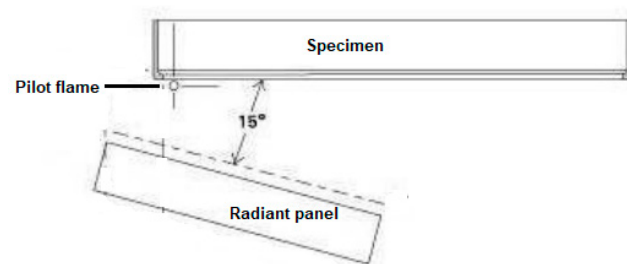


Figure 15. Test configuration scheme.

Following ignition, any flame front that develops is noted, and a record is made of the progression of the flame front along the specimen length, which was previously traced with marks every 50 mm.

Figure 16a shows a sample of the Metasolution under testing, and Figure 16b shows the specimen after the test. The Metasolution was damaged (partially charred, not melted) within the first 50 mm from the hot end, while for the remaining length the sample appears to be intact. Moreover, the sample never showed fire ignition.

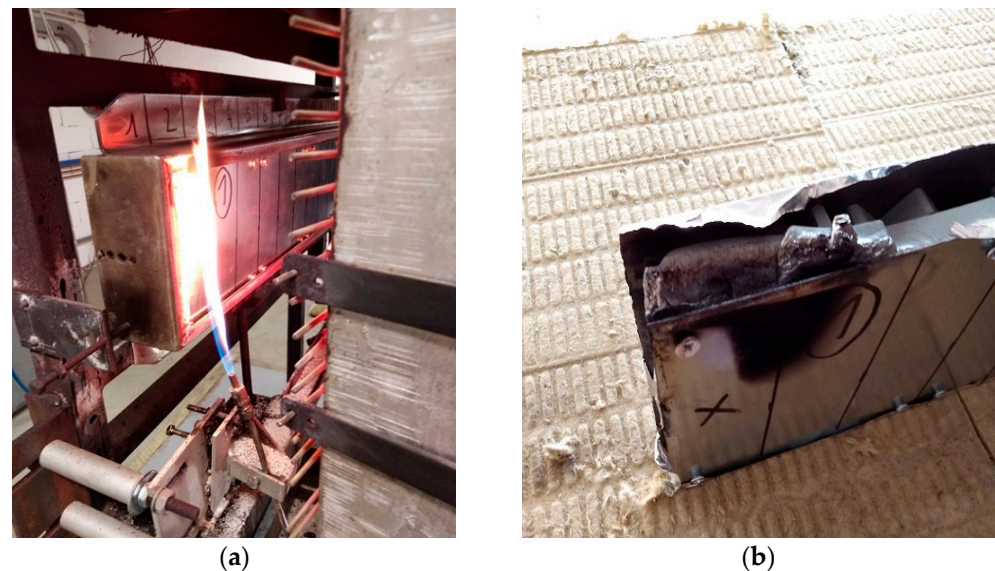


Figure 16. (a) Flame application on the second sample typology with the first layer in the metallic plate and (b) sample after the test.

In Table 4 the values of parameters (CFE = critical flux at extinguishment, Qsb = heat for sustained burning, Qp = peak heat release rate, Qt = total heat release) required by the FTP Code [29] are reported together with the imposed limits. It is evident that the Metasolution, even if tested in the worst case (with the elastic elements in plastic), satisfies the safety regulations.

Table 4. Resulting parameters of surface flammability test.

Sample	CFE [kW/m ²]	Qsb [MJ/m ²]	Qp [kw]	Qt [MJ]	Burning Drops
Limit	≥20	≥1.5	≤0.7	≤0.7	0
Sample 1	50.5	∞	0	0	0
Sample 2	50.5	∞	0	0	0
Mean	50.5	∞	0	0	0

CFE: critical flux at extinguishment; Qsb: heat for sustained burning; Qp: peak heat release rate; Qt: total heat release.

6. Conclusions

In this paper, an eco-sustainable solution to replace traditionally adopted solutions on board ships to reduce transmitted noise through cabin ceilings was presented. The Metasolution investigated, being made only with steel parts, is a valid replacement and a reasonable green alternative to noise-absorbing panels mostly made of mineral wools.

The systematic FE analysis performed to design the Metasolution identified the optimal solution described by the parameters given in Table 3. This particular configuration, tested in the double chamber, shows an advantage of 6 dB in terms of R_w , compared with the benchmark panel. Moreover, Figure 10 shows that the Metasolution has a better performance than the benchmark solution in terms of STL, in the overall frequency range investigated (100–5000 Hz), with the exception of the 100–160 Hz interval.

Other authors have studied similar solutions [19–21] numerically and theoretically in the aeronautical field; however, the Metasolution, the first application of metamaterials in the naval field, was also analyzed experimentally in the laboratory and tested under real conditions, proving that it conforms with normative ISO [22–25] and IMO [28] standards. With respect to the core for sandwich panels proposed by other authors, the Metasolution responds to the need for an easier industrialization and production alternative. Unlike the panels studied in the aeronautical field, mainly designed to guarantee high stiffness, the design of the Metasolution has been studied to obtain a trade-off between stiffness (to ensure self-standing capacity) and acoustic performance in the medium–low frequency range.

The production cost for the Metasolution panel is aligned with the cost of traditional panels mounted on board ships. Moreover, the use of a compact integrated panel of 40 mm height leads to saving space and to a straightforward installation procedure, not impaired by the 2.5 kg/m² weight increase.

The validity of the Metasolution as an alternative method of soundproofing was proven on a mock-up of a ship's deck structure simulating the operational environment. The results showed that the calculated R_w was comparable with that obtainable with a traditional under-deck ceiling system.

The fire tests performed according to the FTP Code showed that the proposed solution entirely respects the safety regulations for installation on board ships, as explained in Table 4.

To conclude, the panel has suitable characteristics to be a valid eco-sustainable solution for noise control on board ships, as an alternative to traditional mineral wool products. This type of solution could pave the way for the substitution of traditional solutions for vibration and noise control in other configurations in the marine field.

Author Contributions: Conceptualization, L.D., S.C. and G.K.O.D.; methodology, S.C. and L.D.; software, S.C. and L.D.; data curation S.C. and L.D.; writing—original draft preparation, S.C., G.R., and G.K.O.D.; writing—review and editing S.C., G.K.O.D. and G.R.; supervision, L.D. and M.B.; project administration, L.D. and M.B. All authors have read and agreed to the published version of the manuscript.

Funding: The research was performed inside the project “Silent Ceiling” financed by Fincantieri SpA for the study of ceiling acoustic insulation systems for public areas onboard cruise ships. The project was carried out in collaboration with the companies CSNI Scarl and Phonic Vibes.

Institutional Review Board Statement: Not applicable.

Informed Consent Statement: Not applicable.

Data Availability Statement: Not applicable.

Acknowledgments: The authors would like to thanks Eng. Enrico Lembo, supervisor of the project for Fincantieri, and Eng. Emanuele Brocco, coordinator of the project for CSNI Scarl, for sharing the data and the obtained results.

Conflicts of Interest: The authors declare no conflict of interest.

References

1. Norton, M.P.; Karczub, D.G. *Fundamentals of Noise and Vibration Analysis for Engineers*, 2nd ed.; Cambridge University Press: Cambridge, UK, 2003; ISBN 0521499135.
2. Fahy, F.; Thompson, D. (Eds.) *Fundamentals of Sound and Vibration*, 2nd ed.; CRC Press/Taylor & Francis Group: Boca Raton, FL, USA, 2015; ISBN 978-0-415-56210-2.
3. de Melo Filho, N.G.R.; Van Belle, L.; Claeys, C.; Deckers, E.; Desmet, W. Dynamic Mass Based Sound Transmission Loss Prediction of Vibro-Acoustic Metamaterial Double Panels Applied to the Mass-Air-Mass Resonance. *J. Sound Vib.* **2019**, *442*, 28–44. [\[CrossRef\]](#)
4. Gazzola, C.; Caverni, S.; Corigliano, A. From Mechanics to Acoustics: Critical Assessment of a Robust Metamaterial for Acoustic Insulation Application. *Appl. Acoust.* **2021**, *183*, 108311. [\[CrossRef\]](#)
5. Langfeldt, F. Membrane-Type Acoustic Metamaterials for Aircraft Noise Shields. Ph.D. Thesis, TUHH Universitätsbibliothek, Hamburg, Germany, 2018.
6. Langfeldt, F.; Gleine, W.; von Estorff, O. Enhancing the low-frequency noise reduction of a double wall with membrane-type acoustic metamaterials. In Proceedings of the Inter-Noise 2016, Hamburg, Germany, 21–24 August 2016; pp. 7551–7562.
7. Isaac, C.W.; Pawelczyk, M.; Wrona, S. Comparative Study of Sound Transmission Losses of Sandwich Composite Double Panel Walls. *Appl. Sci.* **2020**, *10*, 1543. [\[CrossRef\]](#)
8. Hussein, M.I.; Leamy, M.J.; Ruzzene, M. Dynamics of Phononic Materials and Structures: Historical Origins, Recent Progress, and Future Outlook. *Appl. Mech. Rev.* **2014**, *66*, 040802. [\[CrossRef\]](#)
9. de Melo Filho, N.G.R.; Claeys, C.; Deckers, E.; Desmet, W. Realisation of a Thermoformed Vibro-Acoustic Metamaterial for Increased STL in Acoustic Resonance Driven Environments. *Appl. Acoust.* **2019**, *156*, 78–82. [\[CrossRef\]](#)
10. Laude, V. *Phononic Crystals Artificial Crystals for Sonic, Acoustic, and Elastic Waves*, 2nd ed.; De Gruyter: Berlin, Germany, 2020; ISBN 9783110641189.
11. Ma, G.; Sheng, P. Acoustic Metamaterials: From Local Resonances to Broad Horizons. *Sci. Adv.* **2016**, *2*, e1501595. [\[CrossRef\]](#) [\[PubMed\]](#)
12. Morandi, F.; Miniaci, M.; Guidorzi, P.; Marzani, A.; Garai, M. Acoustic Measurements on a Sonic Crystals Barrier. *Energy Procedia* **2015**, *78*, 134–139. [\[CrossRef\]](#)
13. Al Ba'ba'a, H.; Attarzadeh, M.A.; Nouh, M. Experimental Evaluation of Structural Intensity in Two-Dimensional Plate-Type Locally Resonant Elastic Metamaterials. *J. Appl. Mech.* **2018**, *85*, 041005. [\[CrossRef\]](#)
14. An, X.; Fan, H.; Zhang, C. Elastic Wave and Vibration Bandgaps in Two-Dimensional Acoustic Metamaterials with Resonators and Disorders. *Wave Motion* **2018**, *80*, 69–81. [\[CrossRef\]](#)
15. Langfeldt, F.; Gleine, W.; von Estorff, O. An Efficient Analytical Model for Baffled, Multi-Celled Membrane-Type Acoustic Metamaterial Panels. *J. Sound Vib.* **2018**, *417*, 359–375. [\[CrossRef\]](#)
16. Yang, M.; Sheng, P. Sound Absorption Structures: From Porous Media to Acoustic Metamaterials. *Annu. Rev. Mater. Res.* **2017**, *47*, 83–114. [\[CrossRef\]](#)
17. Li, J.; Wen, X.; Sheng, P. Acoustic Metamaterials. *J. Appl. Phys.* **2021**, *129*, 171103. [\[CrossRef\]](#)
18. Kumar, S.; Lee, H.P. Labyrinthine Acoustic Metastructures Enabling Broadband Sound Absorption and Ventilation. *Appl. Phys. Lett.* **2020**, *116*, 134103. [\[CrossRef\]](#)
19. Wang, D.-W.; Ma, L.; Wang, X.-T.; Qi, G. Sound Transmission Loss of Sandwich Plate with Pyramidal Truss Cores. *J. Sandw. Struct. Mater.* **2020**, *22*, 551–571. [\[CrossRef\]](#)
20. Fu, T.; Chen, Z.; Yu, H.; Zhu, X.; Zhao, Y. Sound Transmission Loss Behavior of Sandwich Panel with Different Truss Cores under External Mean Airflow. *Aerosp. Sci. Technol.* **2019**, *86*, 714–723. [\[CrossRef\]](#)
21. Wang, D.-W.; Ma, L.; Wen, Z.-H. Sound Transmission through a Sandwich Structure with Two-Layered Pyramidal Core and Cavity Absorption. *J. Sound Vib.* **2019**, *459*, 114853. [\[CrossRef\]](#)
22. MSC 91/22/Add.1 Adoption of the Code on Noise Levels on Board Ships; International Maritime Organization (IMO): London, UK, 2014.
23. ISO 15186-1; Acoustics—Measurement of Sound Insulation in Buildings and of Building Elements Using Sound Intensity—Part 1: Laboratory Measurements. International Organization for Standardization (ISO): Geneva, Switzerland, 2000.
24. ISO 15186-2; Acoustics—Measurement of Sound Insulation in Buildings and of Building Elements Using Sound Intensity—Part 2: Field Measurements. International Organization for Standardization (ISO): Geneva, Switzerland, 2000.
25. ISO 717-1; Acoustics—Rating of Sound Insulation in Buildings and of Building Elements—Part 1: Airborne Sound Insulation. International Organization for Standardization (ISO): Geneva, Switzerland, 2020.
26. Comsol, Acoustics Module Users Guide. Available online: <https://doc.comsol.com/5.3/doc/com.comsol.help.aco/AcousticsModuleUsersGuide.pdf> (accessed on 8 May 2022).
27. Bonfiglio, P.; Pompili, F.; Lioni, R. A Reduced-Order Integral Formulation to Account for the Finite Size Effect of Isotropic Square Panels Using the Transfer Matrix Method. *J. Acoust. Soc. Am.* **2016**, *139*, 1773–1783. [\[CrossRef\]](#) [\[PubMed\]](#)
28. IMO. *International Code for Application of Fire Test Procedures (FTP Code), Annex 1, Appendix 1*; International Maritime Organization (IMO): London, UK, 2010.
29. IMO. *International Code for Application of Fire Test Procedures (FTP Code), Annex 1, Part 5*; International Maritime Organization (IMO): London, UK, 2010.
30. ISO 5658-2; Reaction to Fire Tests—Spread of Flame—Part 2: Lateral Spread on Building and Transport Products in Vertical Configuration. International Organization for Standardization (ISO): Geneva, Switzerland, 2006.